JOURNAL OF MATERIALS SCIENCE **35** (2000) 3849–3855

Effects of additives on densification, microstructure and properties of liquid-phase sintered silicon carbide

D. SCITI, A. BELLOSI
CNR-IRTEC, Via Granarolo 64, Faenza, Italy
E-mail: bellosi@irtec1.irtec.bo.cnr.it

Dense SiC ceramics were obtained by hot pressing of β-SiC powders using Al_2O_3-Y_2O_3 and La_2O_3-Y_2O_3 additive systems. The effect of the addition of an amount of ultrafine SiC to commercial silicon carbide powder was evaluated. Sintering behaviour and microstructure depended on type and amount of liquid phase, as densification proceeded via a classical solution-reprecipitation mechanism. A core/rim structure of SiC grains indicated that reprecipitation of a solid solution of SiC containing Al and O occurred on pure SiC nuclei. Grain boundary phase was constituted of crystalline YAG and amorphous silicates. Values of flexural strength up to ~750 MPa at RT and up to ~550 MPa at 1000 °C were measured. At 1300 °C a strong degradation of strength was attributed to softening of the amorphous portion of grain boundary phase. In highly dense materials toughness ranged from 2.95 to 3.17 MPa·$m^{1/2}$ and hardness from 21 to 23 GPa.

1. Introduction

SiC ceramic is one of the promising candidate materials for high temperature structural components in heat engines, heat exchangers, wear resistant components, etc. Silicon carbide is difficult to densify without additives, because of covalent nature of Si-C bonding and low self-diffusion coefficient [1]. Solid state sintering, with addition of boron and carbon, at temperatures around 2100 °C has become a routine process to densify silicon carbide. However these materials are characterized by a coarse microstructure and strength values lower than 400 MPa, due to reduced flaw tolerance caused by the low fracture toughness [1]. Liquid-phase sintered silicon carbide (LPS-SiC) [2–7] has the potential to become an alternative, commercially attractive material, which can be densified at lower temperatures (1750–2000 °C). Addition of metal oxides results in liquid phase formation at elevated temperatures, which acts as a mass transport media during sintering. The most important factors which influence liquid phase sintering of SiC are [8–17]: characteristics of the starting powders (grain size distribution and oxygen and carbon content), sintering method and related parameters (time, temperature, pressure), sintering atmosphere (vacuum, argon, nitrogen), amount and composition of liquid phase, use of a powder bed and its composition, processing methods prior to firing. A number of different sintering aids have been used, e.g. alumina and rare earth oxides; sintering mechanisms have been proposed dependent upon each particular additive system. The major requirements on the liquid phase sintering medium are: a sufficient volume fraction of liquid exhibiting complete wetting of the solid phase and an appreciable solubility of the solid in the liquid. The transport properties of the liquid phase depend on its volume fraction and chemistry and these factors are influenced by the selected additives and densification parameters. Densification behaviour and grain growth during liquid phase sintering can be controlled through fabrication parameters. By means of controlled processes, nearly full densities and homogeneous and fine microstructures can be obtained. These microstructures do not contain the large SiC grains which generally are present in solid state sintered silicon carbides and act as stress concentrators. Compared to solid state sintered SiC, LPS-SiC has a room temperature strength that is twice as high [2, 6]. Relationships between toughening behaviour and microstructure are reported [8–10, 14, 18–27]. Mechanical and chemical properties of LPS-SiC ceramics are also strongly affected by intergranular microstructure, which can be a glassy or a partially crystalline phase as residue of the liquid sintering medium. At high temperatures, glass softens and generally decreases all high temperature mechanical and chemical properties. In this respect composition and amount of grain boundary phases are of paramount importance and improvement in properties can be achieved through a careful design of microstructure [6, 10–14, 27–32] and development of innovative processing routes [17, 33].

This paper aims to draw relationships among compositions, microstructure and mechanical properties of nearly-fully dense LPS-SiC ceramics. Several additive systems were selected, in amounts from 6 to 10 wt %. The effect of an addition of ultrafine SiC powder to commercial SiC was tested too. Densification was

TABLE Ia Starting compositions of SiC + additives

Sample	Composition	Amount of additives (wt %)	Ratio SiO_2/additives	Amount of SiO_2 (wt %)
SAY64	SiC + 6wt % Al_2O_3 + 4wt % Y_2O_3	10	0.15	1.49
SAY32	SiC + 3.6wt % Al_2O_3 + 2.4wt % Y_2O_3	6	0.26	1.55
SAY33	SiC + 3.29wt % Al_2O_3 + 3.41wt % Y_2O_3	6.7	0.23	1.54
SAY23	SiC + 2.66wt % Al_2O_3 + 3.45wt % Y_2O_3	6.1	0.14	0.86*
SSAY64	SiC + 6wt % Al_2O_3 + 4wt %Y_2O_3 + 18wt % SiC ultrafine	10	0.23	2.29
SLY33	SiC + 3wt % La_2O_3 + 3wt % Y_2O_3	16	0.26	1.55

*The amount of silica in the starting powder was reduced from 1.65 to 0.92 wt % with a thermal treatment at 1200 °C under argon.

TABLE Ib Grain boundary phase composition

	Al_2O_3		Y_2O_3		SiO_2	
Sample	wt %	mol %	wt %	mol %	wt %	mol %
SAY64	52.0	58.0	35.0	17.5	13.0	24.5
SAY32	47.6	49.0	31.7	15.0	20.5	36.0
SAY33	40.0	44.0	41.0	21.0	19.0	35.0
SAY23	38.0	47.0	50.0	27.0	12.0	26.0
SSAY64	48.8	51.3	32.5	15.5	18.6	33.2
SLY33	La_2O_3		Y_2O_3		SiO_2	
	40.0	46.0	40.0	14.0	20.0	40.0

carried out by hot pressing and the sintering behaviour was studied on shrinkage curves.

2. Experimental procedures

Starting from the following SiC powders:

– Commercial powder, Starck BF-12: 97% β-SiC and 3% α-SiC, s. s. a. 11.6 m^2/g, chemical composition: C = 30.21%, O = 0.88%, Fe = 340 ppm, Al = 210 ppm, Ca = 15 ppm, silica ∼1.65 wt % (estimated from the amount of oxygen);

– SiC ultrafine powder synthesized through laser-induced reaction (Enea-Frascati, Italy): 100% β-SiC, s. s. a. 42 m^2/g, chemical composition: C = 29%, O = 3.4%, silica 6.1 wt % (estimated from the amount of oxygen);

different compositions (Table I) were prepared using as additive powders: Al_2O_3 (Baikalox CR30), Y_2O_3 (HC-Starck) and La_2O_3 (Merck).

The powder mixes were prepared using a pulsed ultrasonic method in ethyl alcohol, drying at 80 °C in rotary evaporator and sieving. All mixes were densified through hot pressing at 1880 °C, 30 MPa, for 20–60 min. Microstructure of hot pressed materials was analyzed on fracture, polished, plasma etched surfaces, by scanning electron microscopy and microanalysis. Phase analysis was determined by X-ray diffraction. The following mechanical properties were measured: Vickers hardness ($H\nu$) obtained using a load of 1.0 Kg, fracture toughness (K_{Ic}) by the Direct Crack Measurement (DCM) method with a load of 10 Kg, using the formula proposed by Anstis *et al.* [34], Young's modulus (E) by the resonance frequency method on samples 28 × 8 × 0.8 mm, and strength (σ) up to 1300 °C by the 4-pt method on 2 × 2.5 × 25 mm (inner span 10 mm, outer span 20 mm).

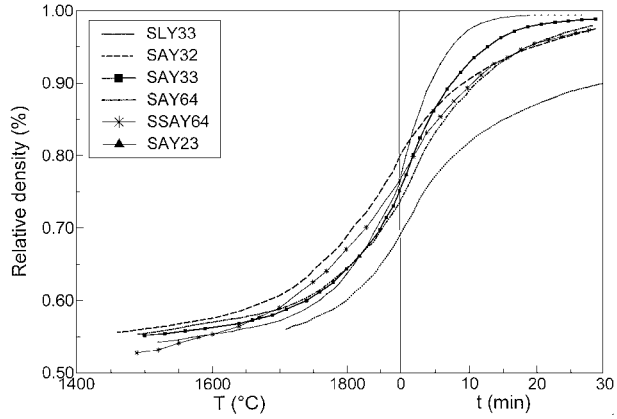

Figure 1 Hot pressing densification behaviour: relative density vs *temperature* during heating up stage and vs *time* during isothermal stage.

3. Results and discussion

3.1. Densification behaviour

Hot pressing cycles were performed at 1880 °C, 30 MPa, under vacuum, with soaking times ranging from 20 to 60 min (Table II). Some parameters indicating the densification behaviour and microstructural characteristic of the dense hot pressed materials are also shown in Table II.

The starting relative density was similar for all samples, in the range 54–56%. All powder mixes containing $Al_2O_3 + Y_2O_3$ as sintering aids, independently of their total and relative amounts, started to densify at 1470–1520 °C and reached high densities (>98%), while the mixture containing $Y_2O_3 + La_2O_3$ started to densify at 1710 °C and reached a final relative density of ∼94%. The densification behaviour, shown in Fig. 1, was strictly dependent on the characteristics of the liquid phase resulting from reaction at high temperature between sintering aids and silica present in the starting powders. The ratio silica/sintering aids influenced the temperature at which densification started (Tables I and II), which was assumed as the beginning of liquid phase formation.

In systems containing $Y_2O_3 + Al_2O_3$, although compositions SAY64 and SAY32 corresponded to the lowest eutectic (1780 °C) in Y_2O_3-Al_2O_3 phase diagram [35], the presence of silica lowered the temperature of liquid phase formation. Considering the Y_2O_3-Al_2O_3-SiO_2 phase diagram [36], eutectic temperature as low as 1400 °C can be found. The relative presence of silica was more relevant in sample SAY32 than in SAY64, due to the reduced amount of additives (from 10 wt % to 6 wt %). The composition of additives in SAY23

TABLE II Hot pressing conditions: $T = 1880\,^{\circ}C$ $P = 30$ MPa., t: soaking time. Parameters describing sintering behaviour: T_0: temperature at which densification starts (particle rearrangement), T_1: temperature at which 2° densification stage (solution/diffusion/reprecipitation) starts, D: density at 1880 °C, D_f: final density, $d\rho/dt_{0.85}$: densification rate at 85% relative density, $1/n$: value of the exponent related to rate controlling mechanism during second densification stage. Microstructural features: d: mean grain size, crystalline phases (besides β-SiC and traces of α-SiC)

Sample	H.P, t min	T_0 °C	T_1 °C	D%	D_f %	D_f g/cm^3	$d\rho/dt_{0.85}$ *10^{-4} g cm^{-3} s^{-1}	$1/n$	d μm	Crystal. phases vol %	Amorph. silicate wt%
SAY64	20	1490	1780	73	98.5	3.24	5.7	1/5.7	0.54	5 YAG	4
SAY32	40	1470	1725	80	99.0	3.21	8.6	1/10	0.56	3 YAG	3.3
SAY33	30	1500	1790	75	99.4	3.24	9.8	1/6	0.59	4 YAG	2.3
SAY23	30	1520	1760	77	99.4	3.24	15.7	1/6.8	0.63	4 YAG	traces
SSAY64	35	1480	1725	76	97.8	3.22	5.8	1/8	0.48	5 YAG	5.3
SLY33	60	1710	1820	68	94.2	3.11	2.6	1/5	0.78	5 Y/La-Si-O	-

corresponded to the stoichiometric ratio of alumina and yttria necessary to form YAG phase ($3Y_2O_3.5Al_2O_3$), moreover, in order to limit the influence of silica, a thermal treatment was carried out to reduce silica in the starting powder to a value of 0.92 wt %. In our samples, the liquid phase started to form at the beginning of shrinkage (T_0 in Table II), but the formation of liquid phase was supposed to be complete at the temperature (T_1), which corresponded to the beginning of second densification stage. As expected, the system containing $Y_2O_3 + La_2O_3$ was highly refractory, being 1750 °C the eutectic temperature observed in the phase diagram [36, 37]. In our case, the presence of silica in SiC powder lowered this temperature to about 1710 °C.

When an amount of liquid phase forms in a green powder sample, densification is presumed to result from flux of matter through the contact region to the surface of the necks between solid particles. This particle drawing is aided by formation of a liquid phase. Afterwards, when large amounts of liquid form, wet and penetrate among solid particles, these are quickly rearranged by sliding over one another with little friction among them. At the same time, as the solid is partially soluble in the liquid (up to carbon saturation of the melt), the solution-diffusion-reprecipitation mechanism determines the fast densification detected in the second densification stage. Densification rates calculated for relative densities of 0.85 (Table II) ranged from 2.6 (in sample SLY33 which had the most refractory liquid phase) to 15.7 g/cm^{3}s^{-1} (sample SLY23: liquid phase corresponding to YAG composition): these values depended on viscosity and amount of liquid phase. According to Kingery's liquid phase sintering model [38], second stage densification kinetics (solution-diffusion-reprecipitation) under isothermal conditions can be described by the equation $\Delta L/L_0 = kt^{1/n}$, where $\Delta L/L_0$ represents the shrinkage during densification and t is the time at processing temperature. The values of $1/n$, related to the particle shape, give indication for the rate controlling densification mechanisms. From our densification data (Fig. 2), considering irregular and prismatic particles in the SiC powder, the second densification stage, up to a relative density of ~95%, seemed to be controlled by diffusion: this being particularly evident for sample SLY33 ($n = 5$) and in satisfactory agreement for samples SAY64, SAY33 and SAY23 where n ranged from 5 to 7. Generally, when diffusion

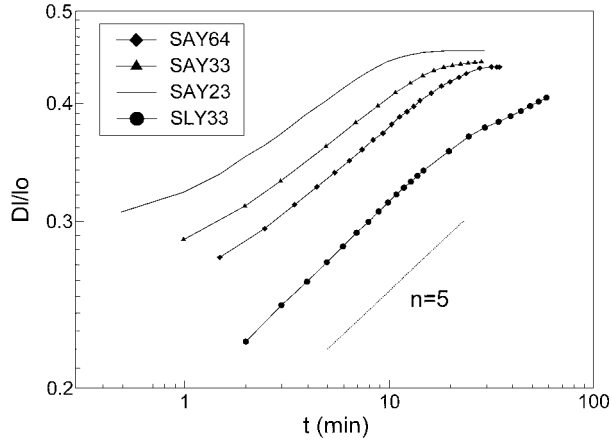

Figure 2 Shrinkage curves of samples SAY64, SAY33, SAY23 and SLY33 vs time during hot pressing isothermal stage.

through liquid phase is the rate-governing step, it accounts for the presence of highly viscous liquid phases. However, it has to be pointed out that an exact definition of the rate controlling mechanism is complicated in the systems under analysis, where solution, diffusion and reprecipitation acted at the same time in liquid phases which were different in composition, distribution, amount and viscosity. In fact, the development of structure and microstructure, i.e. increase in density, formation of grains which have stoichiometries different from pure SiC (as discussed in the following) and grain coarsening, take place with different competitive and overlapped mechanisms.

3.2. Microstructure

The development of microstructure during sintering involves partial solution of the original SiC grains, precipitation around undissolved nuclei and subsequent grain growth. However SiC solubility in the melt is much smaller than in the case of silicon nitride: it was estimated a value lower than 10% [20], but this amount is related to the amount of additives.

Crystalline phases in the hot pressed materials were β-SiC and traces of α-SiC, as in the starting powders. The solution/reprecipitation process did not affect the polytype content. Intergranular crystalline phases were observed corresponding to YAG ($3Y_2O_3{\cdot}5Al_2O_3$) in various amounts up to 5 vol % (Table II). These values, semiquantitatively evaluated from peaks intensities

in X-ray diffractograms, were in agreement with calculations based on the starting compositions. In sample SLY33, crystalline $La_2Si_2O_7$ and $Y_2Si_2O_7$ silicates were detected, for a total amount of about 5 vol %. Beside these crystalline phases, an amount of amorphous phase was supposed to form in all materials owing to reaction of additives with the silica. The estimated amounts of amorphous Al-silicates are shown in Table II for $Al_2O_3 + Y_2O_3$ systems. Our calculation was based on the fact that in all samples except SAY23 there was an excess of Al_2O_3 in respect with the stoichiometric ratio to give crystalline YAG. This amount was considered to combine with SiO_2 to form an amorphous compound as Al_2SiO_5.

Typical microstructural features of the hot pressed materials are shown in Fig. 3a–f. Silicon carbide grains were etched away by a CF_4 plasma, thus microstructures are delineated by grain boundary phases. Grain morphology was mainly equiaxed with grain size distribution ranging from 0.1 to 2 μm. A small number of larger grains (up to 10 μm) with irregular shape, due to the presence of large particle in SiC powder, were detected (Fig. 4). Adjacent SiC grains were mainly separated by a thin grain boundary film, which was the residue of liquid phase sintering medium. Intergranular phases appeared mainly at three- and four-grain pockets: these areas were supposed to be crystalline [31], while amorphous grain boundary phase was presumed

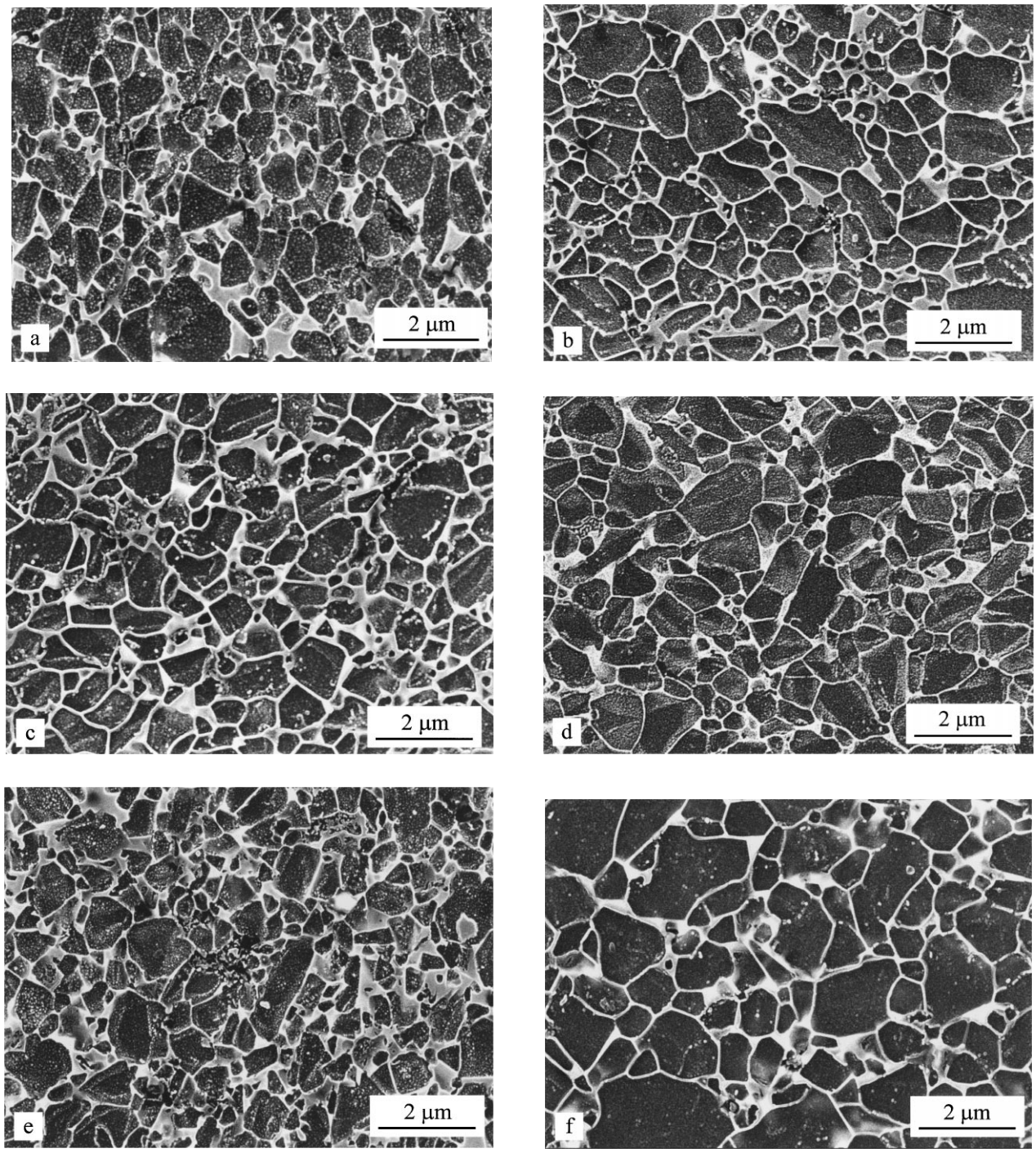

Figure 3 Microstructural features of hot pressed samples: (a) SAY64, (b) SAY32, (c) SAY33, (d) SAY23, (e) SSAY64, (f) SLY33.

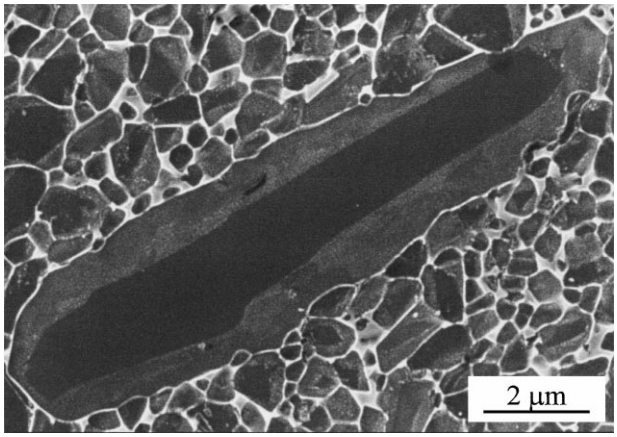

Figure 4 An example of abnormal grain growth in SAY23 sample.

between SiC grains. The pocket sizes, presumably those of YAG phase, increased with increasing amount of additives in the starting powder mixtures. Moreover, the sample produced with an amount of ultrafine SiC powder showed the lowest SiC grain size, but it also seemed to contain the largest size and amount of grain boundary phase pockets; this was due both to the high percentage of sintering aids (the same as sample SAY64) and to the larger amount of silica coming from ultrafine SiC powder. Etched surfaces of samples produced with addition of $Al_2O_3 + Y_2O_3$ revealed a core/rim structure in SiC grains. EDS analyses confirmed variations in core and edge composition. In the core region only Si and C could be detected. In the outer rim, traces of Al and O were observed (Fig. 5), in partial agreement with previous results which claimed the presence of Al, O and Y [31]. This provided evidence that liquid phase sintering of SiC proceeded via a classical solution and reprecipitation mechanism. As sintering started, small SiC grains dissolved into oxide melts until the solubility limit was reached. Then SiC reprecipitated on favourably oriented facets of large undissolved SiC grains, which acted as nucleation sites. Undissolved grains constituted the core and precipitates formed the rim (Fig. 3a–e). The difference in chemical composition between core and rim suggested that SiC with small amounts of Al and O in solid solution was more stable in contact with a Al-Y-O-Si liquid than pure SiC. Smaller SiC grains with rounded shapes were observed in larger pockets of grain boundary phase, while most of the SiC grains developed a faceted interface towards grain boundary phase. This confirmed that, in $Al_2O_3 + Y_2O_3$ additive systems, during densification and grain growth, a reactive Al-Y-O rich liquid phase was present and that surface silica on the starting SiC particles participated in this reaction, as previously observed [32]. The sample containing $LA_2O_3 + Y_2O_3$ showed different microstructural features (Fig. 3f): grain shape was mainly equiaxed and no evidence of a core/rim structure was observed. It confirmed that La-Y-O liquid medium was less reactive than Y-Al-O liquid and that Y and La could not form solid solutions with SiC, probably due to a high ionic radius in comparison with Si. The microstructure of SLY33 showed some defects: areas where porosity located at grain boundaries. The high viscosity of the liquid medium during densification caused difficult wetting of SiC particles surface, and this effect was probably enhanced by scarce reactivity of the liquid with SiC grains: large wetting angles and sharp triangular shapes of grain boundary phase pockets (poor wetting) were in fact observed (Fig. 3f).

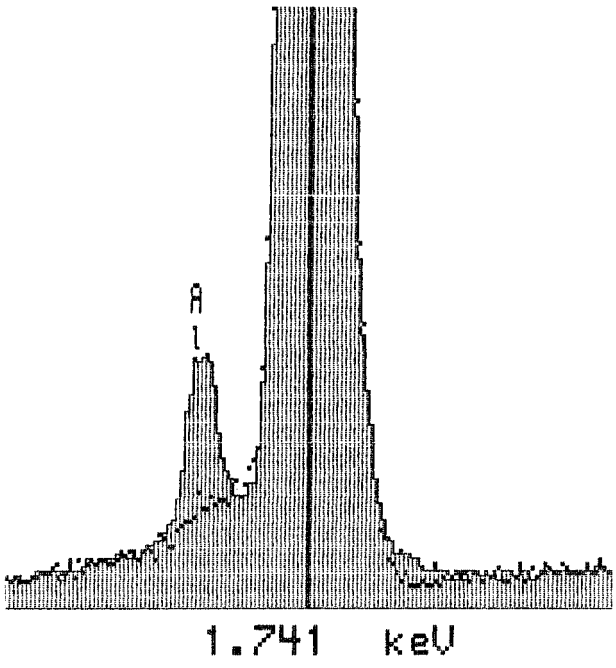

Figure 5 EDS microanalysis showing the presence of Al inside the rim of SiC grains.

3.3. Mechanical properties

High values of hardness (>22 GPa) were measured on all samples (Table III). Fracture toughness was, on the contrary, rather low, due to the characteristics of microstructure and intergranular phases. Cracks, in fact, propagated mainly along grain boundaries but were not appreciably deviated by such a fine and equiaxed grain morphology (Fig. 6a and b). The highest toughness was measured on sample SAY23, where the grain boundary phase was almost completely YAG and the amorphous phase content was very low.

Young's modulus ranged from 383 to 419 GPa, in samples with approximately the same porosity (about 1%): therefore its variation was mainly related to the characteristics of the grain boundary phase, i.e. percentage of crystalline YAG and amorphous phase. In fact sample SAY23, containing a high percentage of YAG, had the highest stiffness. The low Young's modulus measured in sample SLY33 was mainly related to its residual porosity (about 6%).

RT strength values of samples containing $Y_2O_3 + Al_2O_3$ (up to about 750 MPa) were higher than values (300-500 MPa) usually found in solid state sintered SiC and in agreement with results shown in literature on liquid phase sintered SiC [2]. Good strength (up to 536 MPa) was maintained up to ∼1000 °C while it strongly decreased to values lower than 200 MPa at 1300 °C. This strong deterioration was presumably due to softening of amorphous intergranular phase at elevated temperatures. The low values of mechanical

TABLE III Mechanical properties of the hot pressed materials

Sample	density (%)	Hν (GPa)	K_{Ic} (MPam$^{1/2}$)	σ (MPa) RT	σ (MPa) 1000 °C	σ (MPa) 1300 °C	E (GPa)	Flaw size* (μm) I	Flaw size* (μm) II	Flaw size* (μm) III
SAY64	98.5	22.0 ± 0.8	2.97 ± 0.15	746 ± 46	528 ± 53	159 ± 7	386	10	9	7
SAY32	99.0	22.8 ± 0.8	2.95 ± 0.15	658 ± 91	536 ± 37	171 ± 9	391	12	11	8
SAY33	99.4	22.3 ± 1.5	2.95 ± 0.10	712 ± 105	514 ± 66	165 ± 31	404	11	9	10
SAY23	99.4	22.4 ± 1.2	3.17 ± 0.23	656 ± 46	485 ± 36	200 ± 14	419	14	13	10
SSAY64	97.8	22.5 ± 0.9	3.10 ± 0.28	594 ± 53	-	-	383	17	15	11
SLY33	94.2	21.3 ± 1.4	2.68 ± 0.18	420 ± 25	183 ± 36	-	322	25	22	17

*Calculated from Griffith equation, at different flaw shape: I Semicircle c = a, II Semiellipse c = 1.4a, III semiellipse c = 2a.

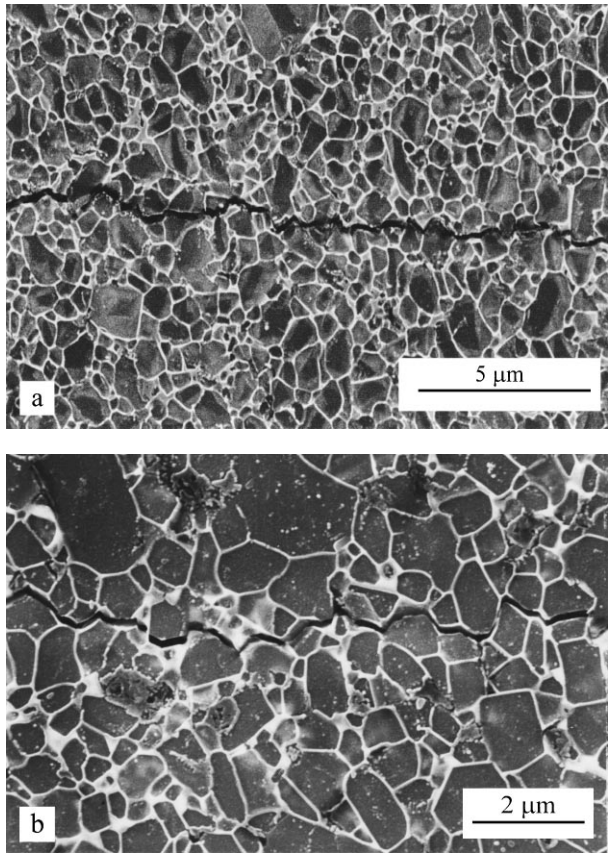

Figure 6 Comparison of crack propagation in samples (a) SAY23 and (b) SLY33.

properties of SLY33 and SSAY64 were due to residual porosity and to microstructural inhomogeneities, respectively.

An estimation of the flaw size C considering different shape factors (semicircular and semielliptical) was performed using Griffith equation $\sigma = YK_{Ic}/C^{1/2}$, where Y is the geometrical factor which depends on flaw shape [39]. The values obtained (Table III) indicated that improvement in strength can be reached through optimization of processing, in order to avoid microstructural inhomogeneities i.e. cracks, voids, aggregates of grain boundary phases.

The addition of an amount of ultrafine SiC powders to commercial powders did not prove useful to improve sinterability and properties.

As a general remark, results on LPS-SiC open the possibility to influence fracture toughness and strength by microstructural design as it is well known for silicon nitride ceramics [40]: additive types and amounts and sintering conditions can be optimized to obtain low amounts of highly refractory crystalline grain boundary phases and in situ-toughened microstructures with elongated grains.

4. Conclusions

Nearly fully dense SiC ceramics were produced by hot pressing at 1880 °C and 30 MPa, through liquid phase sintering with addition of several amounts and compositions of sintering aids in systems $Y_2O_3 + Al_2O_3$ and $Y_2O_3 + La_2O_3$.

Sintering behaviour, microstructure and properties were found to depend on amount and composition of grain boundary phases. High strength values, up to 1000 °C, were obtained but improvement of high temperature strength and of toughness needs further optimization of starting compositions, powders characteristics and processing routes in order to increase the refractoriness of grain boundary phases.

Liquid phase sintering is a useful technique to produce fine grained SiC at a temperature lower of about 200–300 °C than solid state sintered SiC and having tailor-made properties suitable to specific applications.

5. Acknowledgement

The Authors wish to thank F. Monteverde for his helpful contribution in preparation of materials and microstructural analysis, S. Guicciardi and C. Melandri for testing of mechanical properties, D. Dalle Fabbriche for technical assistance, as well as E. Borsella and S. Martelli (ENEA Frascati, Italy) for having provided ultrafine SiC powders.

References

1. K. MOTZFELD, in Proceedings of the International Conference on Engineering Ceramics '92, edited by M. Haviar (Reproprint, Bratislava, 1993) p. 7.
2. W. DRESSLER and R. RIEDEL, *Int. J. Refractory Metals and Hard Materials* **15** (1997) 13.
3. H.-J. KLEEBE, *J. Europ. Ceram Soc.* **10** (1992) 151.
4. F. F. LANGE, *J. Mater. Sci.* **10** (1975) 314.
5. F. K. VAN DIJEN and E. MAYER, *J. Europ. Ceram Soc.* **16** (1996) 413.
6. L. K. FALK, *ibid.* **17** (1997) 983.
7. M. A. MULLA and V. K. KRISTIC, *Ceram. Bull.*, Vol. 70, **3** (1991) 439.
8. S. K. LEE and C. H. KIM, *J. Am. Ceram. Soc.* **77**(6) (1994) 1655.
9. Y.-W. KIM, M. MITOMO, H. EMOTO and J.-G. LEE, *ibid.* **81**(12) (1988) 3136.
10. S. K. LEE, Y. C. KIM and C. H. KIM, *J. Mater. Sci.***29** (1994) 5321.

11. Y.-W. KIM, H. TANAKA, M. MITOMO and S. OTANI, *J. Cer. Soc. Japan, Int. Ed.* **103** (1993) 260.
12. Y.-W. KIM, M. MITOMO and H. HIROTSURU, *J. Am. Ceram. Soc.* **80**(1) (1997) 99.
13. K. LEE, H. H. KIM, E. G. LEE and H. KIM, in "Key Enginering Materials," Vols. 161–163 (Trans Tech Publ. Switzerland, 1999) p. 263.
14. M. MITOMO, *ibid.*, p. 53.
15. G.-D. ZHAN, M. MITOMO, H. SATO and Y.-W. KIM, *ibid.*, p. 243.
16. S. DUTTA, *J. Am. Ceram. Soc.* **68**(10) (1985) C269.
17. J. HOJO, K. MIYACHI, Y. OKABE and A. KATO, *ibid.* **66** (1983) C114.
18. E. LIDEN, E. CARLSTROM, L. EKLUND, B. NYBERG and R. CARLSSON, *ibid.* **78**(7) (1995) 1761.
19. Y.-W. KIM, M. MITOMO and H. HIRITSURU, *ibid.* **78**(11) (1995) 3145.
20. M. J. HOFFMANN and M. NADER, in Engineering Ceramics '96: Higher reliability Through Processing, edited by G. N. Babini *et al.* (Kluwer Academic Publisher, The Netherlands 1977) p. 133.
21. D.-H. KIM and C. H. KIM, *J. Am. Ceram. Soc.* **73**(5) (1990) 1431.
22. K. Y. CHIA and S. K. LAU, *Ceram. Eng. Sci. Proc.* **12**(9-10) (1991) 1845.
23. N. P. PADTURE, *J. Am. Ceram. Soc.* **77**(2) (1994) 519.
24. N. P. PADTURE and B. R. LAWN, *ibid.* **77**(10) (1994) 2518.
25. M. KEPPLER, H.-G. REICHTER, J. M. BROADLEY, G. THURN, I. WIEDMANN and F. ALDINGER, *J. Europ. Ceram. Soc.* **18** (1998) 521.
26. Y.-W. KIM, W. KIM and D.-H. CHO, *J.Mat. Sci. Lett.* **16** (1977) 1384.
27. D.-H. CHO, Y.-W. KI MAND and W. KIM, *J. Mater. Sci.* **32** (1977) 4777.
28. C.-M. WANG and H. EMOTO, *J. Mater. Res.* **12**(12) (1997) 3266.
29. M. MITOMO, Y.-W. KIM and H. HIROTSURU, *ibid.* **11**(7) (1966) 1601.
30. H. YE, V. V. PUJAR and N. P. PADTURE, *Acta Mater.* **47**(2) (1999) 481.
31. L. S. SIGL and H.-J. KLEEBE, *J. Am.Ceram Soc.* **76** (1993) 773.
32. L. K. L. FALK, in Third Euro-Ceramics, Vol. 1, edited by P. Duran and J. F. Fernandez (Faenza Editrice Iberica, 1993) p. 889.
33. S. M. MCMILLAN and R. J. BROOK, in "Ceramic Processing Science and Technology, Ceramic Transaction Vol. 51," edited by H. Hausner *et al.* (The Am. Ceram. Soc., Ohio, 1990) p. 187
34. G. R. ANSTIS, P. CHANTIKUL, B. R. LAWN and D. B. MARSHALL, *J. Am. Ceram Soc.* **64** (1981) 533.
35. E. M. LEVIN and H. F. MC MURDIE, edited by M. K. Raser (The American Ceramic Society, Inc. Columbus, Ohio, 1969) p. 165.
36. *Idem.*, p. 167.
37. E. M. LEVIN and H. F. MCMURDIE, edited by M. K. Reser (The American Ceramic Society, Inc. Columbus, Ohio, 1975) p. 153.
38. W. D. KINGERY, J. M. WOLBROUND and F. R. CHARVAT, *J. Am. Ceram. Soc.* **46** (1963) 391.
39. Y. MURAKAMI, "Stress Intensity Factors Handbook, Vol. 1," (Pergamon Press, Oxford, 1987) p. 42.
40. A. BELLOSI and G. N. BABINI, in "NATO ASI Series, High Technology, Vol. 25, Engineering Ceramics '96," (Kluwer Ac. Publ., Dordrecht, 1997) p. 197.

Received 10 June 1999
and accepted 1 February 2000